Liu *et al. Microstructures* 2024;4:2024061
DOI: 10.20517/microstructures.2024.51

Microstructures

Review

Open Access

Check for updates

Recent advances in preparation, thermoelectric properties, and applications of organic small molecule/SWCNT composites

Peiyao Liu, Yiyang Li, Zhenjie Ni, Cun-Yue Guo

School of Chemical Sciences, University of Chinese Academy of Sciences, Beijing 101408, China.

Correspondence to: Prof. Cun-Yue Guo, School of Chemical Sciences, University of Chinese Academy of Sciences, 19A Yuquan Road, Shijingshan District, Beijing 101408, China. E-mail: cyguo@ucas.ac.cn

How to cite this article: Liu P, Li Y, Ni Z, Guo CY. Recent advances in preparation, thermoelectric properties, and applications of organic small molecule/SWCNT composites. *Microstructures* 2024;4:2024061. https://dx.doi.org/10.20517/microstructures.2024.51

Received: 21 Jun 2024 **First Decision:** 29 Jul 2024 **Revised:** 15 Aug 2024 **Accepted:** 30 Aug 2024 **Published:** 24 Oct 2024

Academic Editors: Zaiping Guo, Zhigang Chen **Copy Editor:** Ting-Ting Hu **Production Editor:** Ting-Ting Hu

Abstract

Thermoelectric materials allow for direct conversion between heat and electricity, realizing a facile and effective utilization of waste heat and thermal management. Semiconductive organic small molecules (OSMs) have attracted ever-increasing attention in thermoelectric device fabrication due to their simplicity in synthesis, well-defined molecular structure, low toxicity, and low thermal conductivity (κ). As a unique one-dimensional (1D) carbon allotrope, single-walled carbon nanotubes (SWCNTs) have excellent structural and electrical properties. Thermoelectric OSM/SWCNT composites with both high conductivity and low thermal conductivity have drawn great attention among researchers and achieved remarkable progress. However, current research fails to give a clear relationship between the structure of small molecules and their thermoelectric performance, and the microscopic mechanisms governing the formation of OSM/SWCNT composites are not well understood as well. These, in all, need further investigation to guide future development in preparing high-performance OSM/SWCNT thermoelectric composites. In this review, we introduce recent advancements in thermoelectric OSM/SWCNT composites, providing a detailed overview of optimization strategies for small molecule dopants. Also summarized in this review article is the design of OSMs from various aspects, including energy level regulation, side chain modification, selection of substituents, etc. Different preparation methods and applications of OSM/SWCNT composites are introduced in detail. Finally, outlooks on the future development of OSM/SWCNT composite thermoelectric materials are pointed out.

Keywords: Organic small molecules, single-walled carbon nanotubes, thermoelectric composites, preparation, properties and applications

INTRODUCTION

Currently, energy scarcity and environmental pollution remain major issues humans are confronted with. Lawrence Livermore National Laboratory estimates that in 2016, the United States consumed about 97.3 quads (quadrillion BTU) of energy, of which about 66% was wasted, mostly in the form of heat[1]. Development in clean energy conversion materials and efficient use of waste heat constitute two big challenges to sustainable development. Thermoelectric materials have the potential to reduce heat pollution to the environment and alleviate energy scarcity by converting heat in various forms into electricity. Research on thermoelectric materials has long been focusing on inorganic semiconductors, including PbTe, Bi_2Te_3, and Sb_2Te_3[2-4], among which Bi_2Te_3 has been put into commercialization[5,6]. However, existing inorganic thermoelectric materials have disadvantages such as expensiveness, toxicity, fragility, complex manufacturing process, and poor bending resistance, which greatly limit their application scenarios[7,8]. Organic thermoelectric (OTE) materials offer several advantages over their inorganic counterparts, including versatile molecular design, simple processing, superior flexibility, non-toxicity, light weight, etc. These merits make OTE materials competitive candidates for new energy materials[9,10]. Although the study of thermoelectric materials dates back to the 19th century, the study of OTE materials has just developed rapidly in the past decade. Additionally, the power factor (PF) of OTE materials has climbed five orders of magnitude in the last few years, and the interest of researchers in these materials has grown rapidly[11-14].

At present, research on OTE materials focuses mainly on conductive polymers and their composites with inorganic constituents. On the one hand, these composites/hybrids currently show better thermoelectric properties[15-18]; on the other hand, polymeric materials have obvious advantages in large-scale preparation and property stability. However, the study of small molecules used for thermoelectric materials is also of great significance. Compared with polymer thermoelectric materials, organic small molecule (OSM) thermoelectric materials have many advantages. Small molecule systems can adapt to more processing methods, have a more definite chemical structure and a simpler and more orderly stacking mode, and can achieve accurate measurement and regulation of physical properties[19,20], so it is more conducive to exploring the relevant mechanism of OTE effect. However, the overall thermoelectric properties of OSMs are low, which hinders their large-scale commercial application. As a one-dimensional (1D) carbon allotrope, single-walled carbon nanotubes (SWCNTs) have excellent electrical and mechanical properties. Although SWCNTs demonstrate high electrical conductivity (σ) of SWCNTs, their high thermal conductivity (κ) is detrimental to thermoelectric performance. They offer distinctive advantages in adjusting carrier density through the use of charge transfer dopants. SWCNT networks often exhibit high porosity and a very large surface area, making them adept at adsorbing redox molecules[21-23], and there will not be any morphological changes when the network is submerged in a range of solvents and dopant-containing solutions. Considering the above conditions, combining OSM semiconductors with SWCNTs to form OSM/SWCNT composite thermoelectric materials is a popular strategy to obtain high thermoelectric performance with high σ and low κ.

This review systematically discusses methods to increase the thermoelectric performance of OSM/SWCNT composite materials from the perspectives of doping, structural design, and solvent selection. It introduces the preparation methods and applications of composite materials, reviews the latest advancements in OSM/SWCNT composite thermoelectric materials, and provides suggestions for future studies and exploration of high-performance OSM/SWCNT composite thermoelectric materials.

THE MAIN PERFORMANCE PARAMETERS OF THERMOELECTRICS

Thermoelectric energy conversion relies on the diffusion movement of carriers to achieve the mutual conversion of heat and electric energy, mainly including three fundamental physical phenomena: the

Seebeck effect, the Peltier effect, and the Thomson effect, collectively known as the thermoelectric effect.

The thermoelectric effect

The Seebeck effect, also known as the first thermoelectric effect, means direct conversion from heat energy into electrical energy. By connecting two different conductor materials with metal, maintaining a certain temperature difference at their ends, and introducing a closed external circuit, an electromotive force can be generated. By utilizing the Seebeck effect, temperature differences in the environment can be converted into potential differences, achieving the goal of thermoelectric power generation[24], as shown in Figure 1A[25]. The Peltier effect is a phenomenon opposite to the Seebeck effect, which lays the theoretical foundation for thermoelectric cooling [Figure 1B][26]. According to Thomson's theory, when a current passes through a uniform conductor with a temperature gradient, in addition to generating joule heat, a certain amount of heat is absorbed or released in order to maintain the original temperature gradient[27]. The Thomson effect can be viewed as a combination of the Seebeck and Peltier effects. Moreover, the three interrelated effects have important applications and significance in the field of thermoelectricity.

Thermoelectric parameters of materials

Abram F. Ioffe proposed a quality factor to describe the comprehensive index of thermoelectric properties of materials, namely the thermoelectric figure of merit (ZT):

$$ZT = S^2\sigma T/\kappa \tag{1}$$

where S, σ, T, and κ represent the Seebeck coefficient, the electrical conductivity, the absolute temperature, and the thermal conductivity, respectively[28].

The electrical conductivity is related to the charge carrier concentration, n, and the charge carrier mobility, μ, through

$$\sigma = ne\mu \tag{2}$$

where e is the elementary charge. Regarding charge transport, high σ necessitates high n and μ. The Hall effect, one of the fundamental magnetoelectric effects, can be used to characterize carrier concentration and mobility. By measuring the Hall voltage of a material, the carrier concentration can be determined. Combined with the material's conductivity σ, the Hall mobility of the material can be calculated using Equation (2). It could be done to investigate high-performing organic semiconductors with high intrinsic carrier mobility as potential sources of superior OTE materials. The Seebeck coefficient is the thermoelectric heat of a semiconductor material and the inherent electron transport characteristic of the material, which can be expressed by:

$$S = \left(\frac{8\pi^2 k_B^2}{3eh^2}\right) m^* T \left(\frac{\pi}{3n}\right)^{2/3} \tag{3}$$

The h and m^* represent the Planck constant and effective mass of carriers, respectively[29]. The S is directly proportional to the m^* and inversely proportional to the n. For a p-type thermoelectric material, its sign of S is positive and the hole is the major charge carrier. In contrast, when the S of thermoelectric material is negative, it indicates n-type thermoelectric material in which the electron transport is predominant. The value of S can be positive or negative, but its magnitude depends on its absolute value. As reflected in Equation (3), to obtain a high S, a large m^* and a small n are required. However, a small n tends to decrease the σ. Therefore, in order to obtain a good thermoelectric material, the σ and S must be regulated to

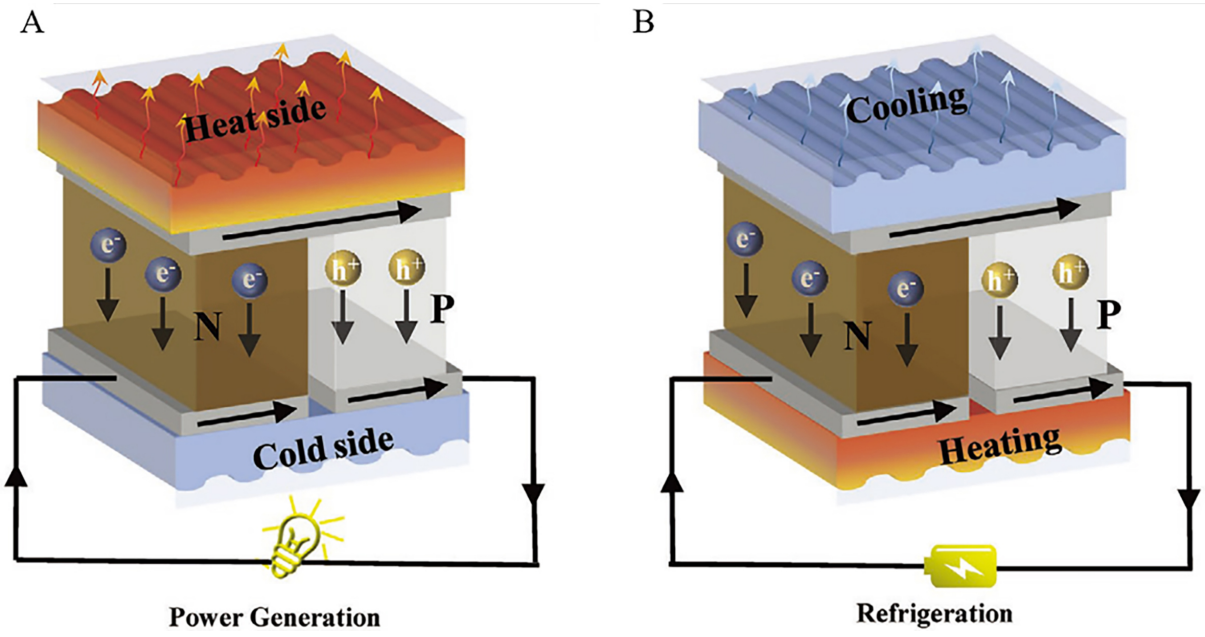

Figure 1. A: Schematic diagram of thermoelectric modules for power generation (the Seebeck effect); B: schematic diagram of thermoelectric modules for refrigeration (the Peltier effect). The figure is quoted with permission from Zhou *et al.*[27].

maximize $S^2\sigma$. Equation (4) reflects that the κ of solid-state materials is primarily composed of two components: the thermal conductivity of the electrons (κ_e) due to carrier-transport behavior and the thermal conductivity of lattice (κ_L) attributed to crystal lattice vibration.

$$\kappa = \kappa_e + \kappa_L \tag{4}$$

$$\kappa_e = L\sigma T \tag{5}$$

Where L is the Lorenz constant. According to Equation (5), κ_e is ignored when the carrier concentration is low. However, when a certain value is reached, the contribution of the carrier to the κ needs to be considered. That is, an increase of the σ value will lead to a corresponding rise of the κ value to a certain extent, thus affecting the overall thermoelectric performance of the material[30].

Improving the thermoelectric performance, that is, increasing ZT, is the core goal pursued in the development of thermoelectric materials. According to Equation (1), a high ZT value requires a high σ, a high S, and a low κ. Electrical conductivity depends on two key parameters: carrier concentration and mobility. The S is closely related to the carrier concentration and density of states (DOS) of the material. Thermal conductivity consists of κ_e and κ_L with the former being directly proportional to carrier concentration. The three parameters determining ZT values are correlated with each other and vary with the carrier concentration. The increase of carrier concentration is conducive to the growth of σ, but at the same time, it will lead to the decrease of S and the increase of κ [Equations (2)-(5)], resulting in a complicated trade-off relationship. Therefore, the highest thermoelectric performance of materials only appears at a specific carrier concentration. In summary, the optimization of ZT is not simply the optimization of a certain parameter, and the interaction between the parameters makes it difficult to improve the overall performance of thermoelectric materials. Since OTE materials are usually used at low temperatures and the range of temperature difference is small, its κ can be considered to remain basically

constant when the temperature changes[31]; the PF is proposed to characterize the capabilities of OTE materials with low κ:

$$PF = S^2\sigma \quad (6)$$

Since PF is closely related to σ and S, based on the above analyses, adjusting carrier concentration to increase σ and S at the same time is an important way to obtain high-performance OTE materials.

STRATEGIES FOR OPTIMIZING TE PROPERTIES OF OSM/SWCNT COMPOSITE MATERIALS

Optimal doping and chemical structure optimization are important ways to enhance the performance of OTE materials. Because the values of the three parameters that make up ZT generally depend on the carrier concentration n in the thermoelectric material [Equations (1)-(3)], the ideal strategy for optimizing the thermoelectric performance is to sensitively adjust the n over a wide range while detecting S, σ, and κ. Through OSM doping, the n of the thermoelectric materials can be precisely adjusted. In OSM/SWCNT composite thermoelectric materials, OSM dopants (in this paper, OSMs equal to dopants) can be used to dope SWCNTs in a simple manner (immersion of SWCNTs in a redox molecular solution) without affecting the network morphology of SWCNTs (e.g., the bridging of SWCNTs, bundle size, etc.) or SWCNTs' electronic structure. In general, SWCNTs typically have p-type thermoelectric properties because of oxygen doping in air, but n-type thermoelectric properties appear after n-type doping. Generally speaking, Brønsted acid or Lewis acid can achieve p-type doping of SWCNTs[23,32,33], while Brønsted base or Lewis base can perform n-type doping[21,22,34,35]. Successful p-type doping requires that the electron affinity of the dopant be greater than the ionization potential of the SWCNTs, whereas n-type doping necessitates that the ionization potential of the dopant be less than the electron affinity of the SWCNTs. The work by Blackburn *et al.* provides a detailed introduction to the application of SWCNTs in thermoelectrics[35]. We will introduce the strategies to optimize the thermoelectric properties of OSM/SWCNT composites from various aspects, focusing on the selection and design of dopant OSMs, including energy level regulation, side chain engineering, substituents, and end group adjustments among others. Additionally, we have summarized the effects of solvents on the thermoelectric performance of OSM/SWCNT materials, as well as design strategies for air-stable n-type thermoelectric materials. The thermoelectric properties of typical OSM/SWCNT composites are summarized in Table 1.

Regulation of OSM energy levels

P-type OSM dopants

Modulation of energy levels of OSMs can significantly enhance the S and PF of OSM/SWCNT composite materials. Reducing the energy barrier between SWCNTs and OSMs benefited energy filtering and maximized thermoelectric performance of the p-type OSM/SWCNT composites. Kim *et al.* reported a series of π-conjugated OSMs [Figure 2A] and their composites with SWCNTs, and the effect of the highest occupied molecular orbital (HOMO) energy levels of OSMs on the thermoelectric performance of OSM/SWCNT composites[36]. When the HOMO energy level of OSMs is similar to the valence band of SWCNT, the S and PF of OSM/SWCNT composites increased significantly compared with those of original SWCNTs. In addition, OSM/SWCNT composites with low barriers have higher thermoelectric properties than composites with high barriers. After that, Kim *et al.* designed three different energy levels and band gaps stilbene derivatives (E)-4,4'-bis[9-(3,6-dimethoxy-9H-carbazolyl)]stilbene (CzS), 4-(3,6-dimethoxy-9H-carbazole-9-yl)-α-[4-(3,6-dimethoxy-9H-carbazole-9-yl)phenyl]methylene-(αZ)-benzenacetonitrile (CzCNS), and 1,2-dicyano-trans-1,2-bis-4-(carbazoylyl)phenylethylene (CzdCNS)[37] [Figure 2B]. The results show that SWCNT/CzS with increased bandgap and decreased barrier energy exhibit enhanced S

Table 1. TE properties of OSM/SWCNT composite materials

Sample	(S cm^{-1})	*S* (μV·K^{-1})	PF (μW·m^{-1}·K^{-2})	*ZT*	Diameter of SWCNTs (nm)	Ref.
SWCNT/KOH/18-crown-6-ether	2050	-33	230	2 × 10^{-3}	-	[21]
CzS/SWCNT	-	108.7	337.2	0.058	-	[37]
Spiro-MeOTAD/SWCNT	-	-	239.2 ± 4.2	-		[39]
SWCNT/dmBT	-	78.5	183.9	-		[36]
SWCNT/dPhiz-6	1671.4 ± 0.2	110.4 ± 2.6	2136	0.13		[38]
SWCNT/onium salt	626	-59.4	221	-	2.0 ± 0.8	[44]
SWCNT/onium salt	703	68.5	330	-	2.0 ± 0.8	[44]
SWCNT/pip	196.0 ± 9.3	-116.7 ± 4.1	267.5 ± 23.6	-		[45]
SWCNT/BBTTPO-F_4TCNQ	3337.3 ± 302.1	33.1 ± 2.8	365.9 ± 15.2		-	[48]
PhBTBT-F_4TCNQ/SWCNT	6660.6	19.2	244.3	-	-	[47]
C8BTBT-F_4TCNQ/SWCNT	520.2	-45.0	105.1	-	-	[47]
SM-Ph-2F/SWCNT	1001.8 ± 166.4	46.5 ± 5.2	214.0 ± 25.8	-	-	[49]
SM-Th-O/SWCNT	1852.4 ± 62.6	40.5 ± 3.0	302.9 ± 20.5	-	-	[49]
SWCNTs/DBOBI-$FeCl_3$	-	-	236.2 ± 12.3	0.021	-	[50]
SWCNT/PyBOP	3731.5 ± 183.5	21.6 ± 0.9	174.0 ± 1.7	-	1-2	[54]
SWCNT/Por-5F	982.4 ± 20.4	53.3 ± 0.4	279.3 ± 9.8		-	[51]
SWCNT/TCzPy	189.4 ± 9.0	75.9 ± 3.3	108.4 ± 4.8	-	-	[52]
SWCNT/ADTAb	642.4 ± 39.2	-44.5 ± 5.0	124.4 ± 10.5	-	1-2	[53]
SWCNT/ADTAg	924.1 ± 45.3	47.8 ± 3.9	211.6 ± 9.9	-	1-2	[53]
SWCNTs/TPETPA	356.2 ± 17.8	123.2 ± 6.8	539.8	-	-	[55]
SFX-2/SWCNT	-	-	218.6	-	-	[57]
SWCNTs/PYB		-48.5	193.6	1.54 × 10^{-3}	1-2	[58]
SWCNT/FcMA	2674.86 ± 136.32	−46.07 ± 0.5	567.54 ± 27.18	-	1-2	[59]
dppf@SWCNT	716	-38	240	-	-	[65]
SWCNT/FcMA/PEG-5%	2299.8 ± 175.6	-	600.6 ± 22.9	-	1-2	[69]

OSM: Organic small molecules; SWCNT: single-walled carbon nanotubes; PF: power factor; CzS: (E)-4,4′-bis[9-(3,6-dimethoxy-9H-carbazolyl)]stilbene; dmBT: 5,5″-(2,5-dimethoxy-1,4-phenylene)bis[2,2′-bithiophene]; BBTTPO: 17-(((4,4″-di([2,2′-bithiophen]-5-yl)-5′-(octadecyloxy)-[1,1′:4′,1″-terphenyl]-2′-yl)oxy)methyl)-13,21-di(2,5,8,11-tetraoxadodecyl)-2,5,8,11,15,19,23,26,29,32-decaoxatritriacontane; F_4TCNQ: tetrafluorotetracyanoquinodimethane; PhBTBT: 2-decyl-7-phenyl[1]benzothieno[3,2-b][1]benzothiophene; DBOBI: 4,7-di([2,2′-bithiophen]-5-yl)-2-(4-octylphenyl)-1H benzo[d]imidazole; TczPy: 1,3,6,8-tetrakis(3,6-di-*tert*-butyl-9*H*-carbazol-9-yl)pyrene; TPETPA: N,N-diphenyl-4′-(1,2,2-triphenylvinyl)-[1,1′-biphenyl]-4-amine; PYB: pyridineborane; PEG: polyethylene glycol.

and PF, leading to a peak room temperature *ZT* of 0.058 for dopant-free thermoelectric (TE) hybrid containing carbon nanotubes (CNTs). SWCNT/CzS has enhanced thermoelectric performance due to lower thermal conductivity and efficient charge carrier transfer. This proves that simultaneously adjusting the bandgap and the HOMO energy level in OSMs can significantly enhance the *S*, thereby maximizing the *ZT* of OSM/SWCNT composites.

Recently, Kim *et al.* designed a series of OSMs by simply optimizing the molecular shape and energy levels of π-OSMs[38]. Figure 2C displays the molecular structure of as-synthesized four OSMs, which are H-shaped π-OSMs with extended aromatic surfaces and twisted phenyl rings. Because of its twisted molecular structure and HOMO energy level, which is similar to that of SWCNTs' valence band, dPhiz-6 may effectively filter out energy between the two materials. With a high *S* of 110.4 ± 2.6 μV·K^{-1}, the composite shows a huge improvement in PF to 2,136 μW·m^{-1}·K^{-1}. Furthermore, via efficient TE transport of the SWCNT/dPhiz-6 composite, its maximum *ZT* exceeds 0.13 at room temperature. This study highlights the

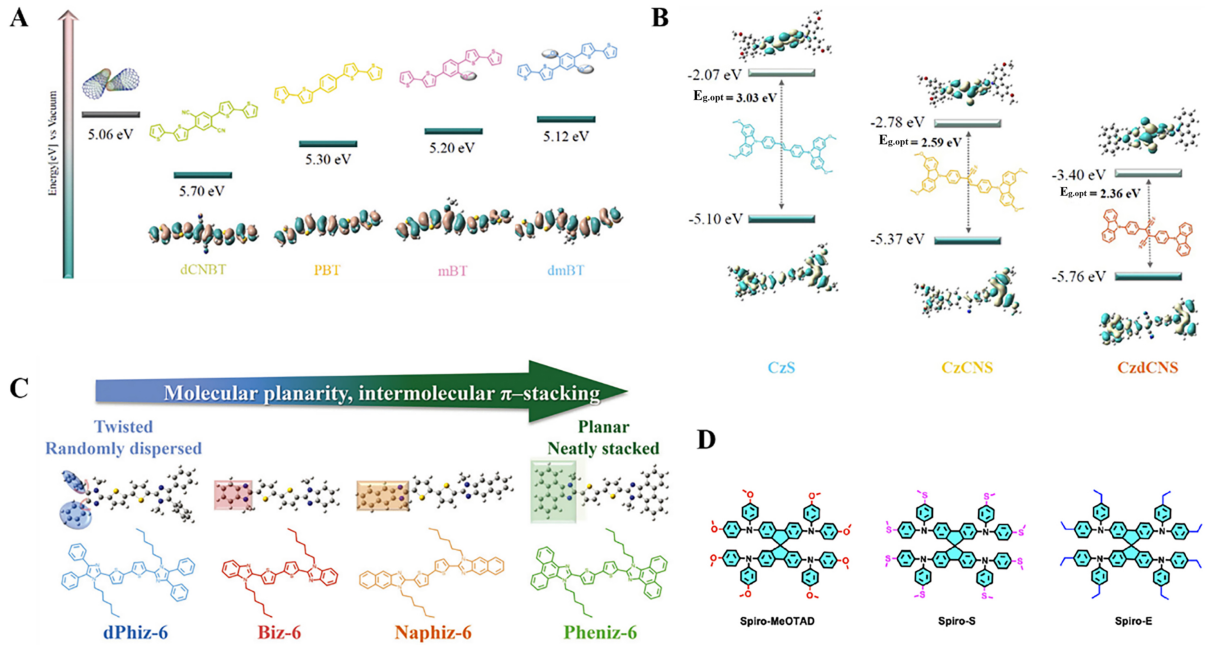

Figure 2. A: Molecular structure and HOMO levels of the four π-conjugated OSMs, The figure is quoted with permission from Kim *et al.*[36]; B: molecular structure, bandgaps and HOMO/LUMO levels of the three stilbene-derivatives, The figure is quoted with permission from Kim *et al.*[37]; C: molecular structures of dPhiz-6, Biz-6, Naphiz-6, and Pheniz-6, The figure is quoted with permission from Kim *et al.*[38]; D: molecular structures of the spiro-bifluorene derivatives, The figure is quoted with permission from Zhu *et al.*[39]. HOMO: Highest occupied molecular orbital; OSMs: organic small molecules; LUMO: lowest unoccupied molecular orbital; dCNBT: 2,5-bis([2,2′-bithiophene]-5-yl)-1,4-benzenedicarbonitrile; PBT: 5,5″-(1,4-phenylene)bis[2,2′-bithiophene]; mBT: 5,5″-(2-methoxy-1,4-phenylene)bis[2,2′-bithiophene]; dmBT: 5,5″-(2,5-dimethoxy-1,4-phenylene)bis[2,2′-bithiophene]; CzS: (E)-4,4′-bis[9-(3,6-dimethoxy-9H-carbazolyl)]stilbene; CzCNS: 4-(3,6-dimethoxy-9H-carbazole-9-yl)-α-[4-(3,6-dimethoxy-9H-carbazole-9-yl)phenyl]methylene-(α Z)-benzenacetonitrile; CzdCNS: 1,2-dicyano-trans-1,2-bis-4-(carbazoylyl)phenylethylene.

molecular engineering optimization of π-OSMs combination with SWCNTs, showcasing the potential for creating the next generation of high-performance thermoelectric materials. Three spiro-bifluorene derivatives were proposed in Zhu *et al.*'s new strategy of p-type doping; the molecular structure is shown in Figure 2D[39]. The energy levels of spiro-difluorene derivatives are altered by the addition of oxygen and sulfur heteroatoms, resulting in HOMO levels that coincide with the Fermi level (E_F) of SWCNTs. The maximum PF of the OSM/SWCNT composite film at ambient temperature is 243.4 $\mu W \cdot m^{-1} \cdot K^{-2}$, which was nearly 108% higher than that of original SWCNTs.

N-type OSM dopants

Typically, an effective n-type doping process achieves electron transfer through two possible pathways[40]: i) direct electron-transfer method, which requires the HOMOs of the dopants to be close to or higher than the lowest unoccupied molecular orbitals (LUMOs) of the host in order for electrons to effectively transfer from the dopant to the host[41]; ii) The hydride transfer induced n-doping between an air-stabilized n-dopant, such as benzimidazole derivatives, and a host with a LUMO level of less than about -4.0 eV[42,43]. However, it is still difficult to precisely manage the OTMs' doping profile in order to maximize the thermoelectric parameters. Yin *et al.* designed four new indacenodithiophene (IDT)-cored OSMs; the molecular structure is shown in Figure 3, and their LUMO levels and energy gaps show a gradient decline, indicating that the n-doping process is becoming easier[40]. Thus, the doping level of IDT/SWCNT hybrid membranes can be controlled through the synergistic effect of primary doping, thereby providing significantly different thermoelectric performances under environmental conditions.

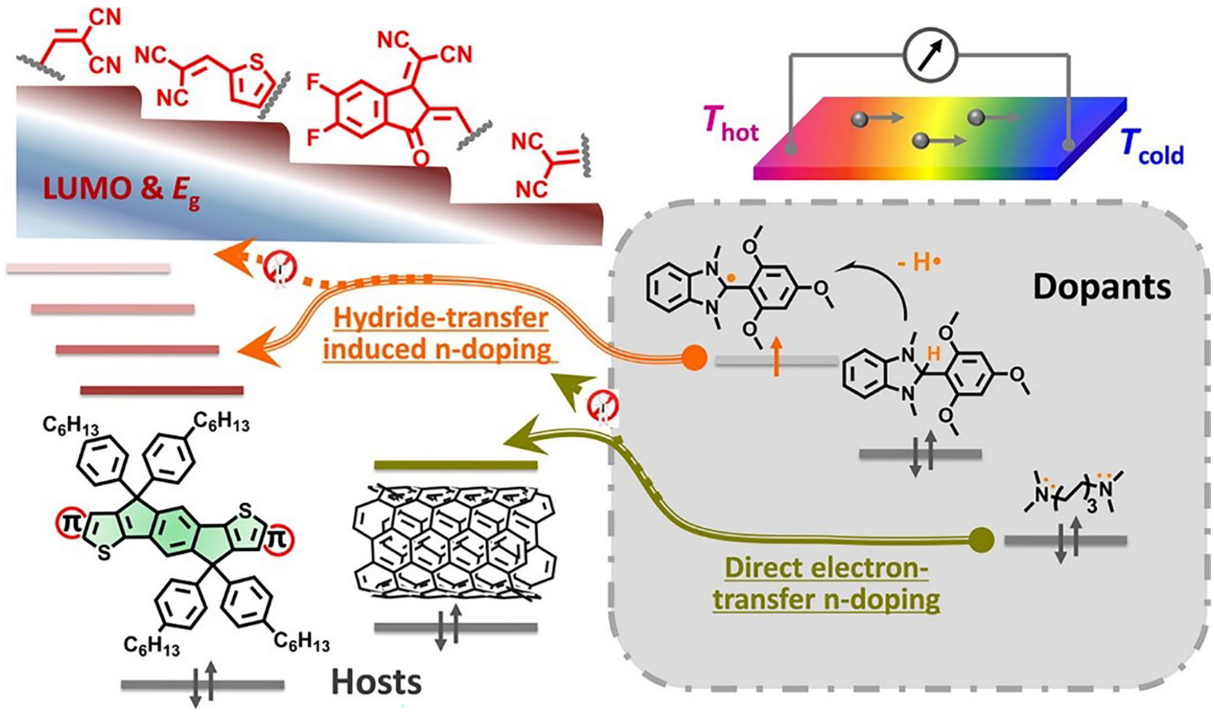

Figure 3. Molecular structure and LUMO levels of the four IDT-cored OSMs. The figure is quoted with permission from Yin *et al.*[40]. LUMO: Lowest unoccupied molecular orbital; IDT: indacenodithiophene; OSMs:organic small molecules.

Sugiura *et al.* systematically studied the control of SWCNT Fermi levels using onium salts as chemical dopants[44]. The findings suggest that cationic substituents and anion affinity of onium salts have great effects on the E_F of SWCNTs. The thermoelectric properties of SWCNTs can be greatly improved by using onium dopants, and the n-type SWCNTs obtained by doping have high stability. Recently, Kim *et al.* regulate the energy levels of n-type OSMs with the addition of two N-ethyl-piperidinyl groups to either side of a core of naphthalenediimide[45]. The resulting composite SWCNT/pip shows a significant enhancement in thermoelectric performance, with maximum PF reaching 291.0 $\mu W \cdot m^{-1} \cdot K^{-2}$. Furthermore, because of the lower LUMO level, the SWCNT/pip composite material demonstrates exceptional environmental endurance. This performance is notably superior to that of traditional n-type OTE materials. These investigations demonstrate that the stability and thermoelectric properties of n-type carbon nanotube (CNT) thermoelectric materials can be significantly improved by designing the energy levels of OSM/SWCNT composites without further doping. Therefore, OSM/SWCNT composites with deep LUMO levels are expected to be promising n-type OTE materials. Such materials have the potential to be ideal components for durable, flexible, and long-lasting p-n TE devices.

Optimizing the structure of OSM dopants

Regulation of side chains

Modifying the side chains of OSM materials is another method to improve thermoelectric performance, which not only increases solubility but also controls molecular packing to generate high carrier mobility[46]. In a previous study, Qin *et al.* reported that [1]benzothieno[3,2-*b*][1]benzothiophene (BTBT) derivatives with different side chains were combined with tetrafluorotetracyanoquinodimethane (F_4TCNQ) to prepare OTE materials with SWCNTs[47]. The effects of side chains on the thermoelectric properties of BTBT derivatives were studied. The 2-decyl-7-phenyl[1]benzothieno[3,2-b][1]benzothiophene (PhBTBT)-F_4 TCNQ/SWCNT composite film exhibits the maximum p-type PF, attributed to its reduced LUMO energy

level effectively absorbing electrons from the SWCNTs' E_F, leading to a raised carrier concentration in the p-type composite film. Based on the composite films with different side chains, a simple thermoelectric generator (TEG) has been prepared with high performance.

Jang *et al.* have produced three rod-coil amphiphilic compounds, 17-(((4,4″-di([2,2′-bithiophen]-5-yl)-5′-(hexyloxy)-[1,1′:4′,1″-terphenyl]-2′-yl)ox-y)methyl)-13,21-di(2,5, 8,11-tetraoxadodecyl)-2,5,8,11,15,19,23,26,29,32-decaoxatritriacontane (BBTTPH), 17-(((4,4"-di([2,2'-bithiophen]-5-yl)-5'-(dodecyloxy)-[1,1':4',1"-terphenyl]-2'-yl)oxy)methyl)-13, 21- di(2, 5, 8, 11-tetraoxadodecyl)-2,5,8,11,15,19,23,26, 29,32-decaoxatritriacontane (BBTTPD), and 17-(((4,4"-di([2,2'-bithiophen]-5-yl)-5'-(octadecyloxy)-[1,1':4',1"-terphenyl]-2'-yl)oxy)methyl)-13,21-di(2,5,8,11-tetraoxadodecyl)-2,5,8,11,15,19,23,26,29,32-decaoxatritriacontane (BBTTPO), each having a distinct alkyl chain[48]. They demonstrated the successful enhancement of thermoelectric performance of OSMs/SWCNT composite films by engineering the alkyl chain of OSMs. The long alkyl chain of BBTTPO increased the bundling of SWCNTs. The findings show that compared to the other two compounds, the thermoelectric performance of SWCNTs-BBTTPO thermoelectric film is higher. This is explained by the fact that SWCNTs-BBTTPO films have a lower tunneling barrier for charge carrier transport. Li *et al.* designed and synthesized three types of OSMs having distinct conjugated main chains and side chains of the identical ionic functional groups[49]. It was found that the attributes of various main chain architectures vary. OSMs with side chains that contain ion functional groups have a special structure that helps them interact with the surface of SWCNTs better, raising the doping level. The highest PF at ambient temperature is 330.2 $\mu W \cdot m^{-1} \cdot K^{-1}$. The benzimidazole backbone was recently chosen as the primary scaffold for OSMs by Jang *et al.*, and they investigated how the OSMs' alkyl chain length affected the thermoelectric performance of OSM/SWCNT hybrids[50]. As the alkyl chain length of OSMs rose from methyl to octyl, the hybrids' *S* improved as well. Additionally, the expansion of the alkyl chains reduced the likelihood that the OSM/SWCNT hybrids' electrical conductivity would be sacrificed. This is caused by the complementary effects of OSM/SWCNT's suitable potential barrier and the smaller diameter of SWCNT bundles, which encourage effective carrier transport and energy-dependent carrier scattering, respectively. According to the findings, doping with 4,7-di([2,2'-bithiophen]-5-yl)-2-(4-octylphenyl)-1H benzo[d]imidazole (DBOBI) significantly increased the PF of SWCNTs. Additionally, the PF of the OSM/SWCNT hybrids can be raised even further by optimizing the charge carrier concentration.

Substitution groups and terminal adjustments

The structure of substituents and terminals also greatly influences the thermoelectric properties of OSMs. Zhou *et al.* created and synthesized five porphyrin-based OSMs as potential p-type thermoelectric materials[51]. A new strategy has been proposed to adjust the structure and thermoelectric property relationship by altering the peripheral substituents of porphyrins. The hydrophobic porphyrin-based hybrid membranes show significant enhancements in σ and PF values. It was found that introducing hydrophobic groups on the porphyrin skeleton significantly affects the charge carrier mobility by influencing the distribution of SWCNTs, which is essential for enhancing σ value. Yin *et al.* created and synthesized four OSMs as strong p-type thermoelectric materials, and they also examined the structure-thermoelectric performance relationship, specifically the conjugated backbone and peripheral substituents[52]. The band gap and HOMO level of OSM essentially influence the electric field in the SWCNT-hybrid system, thereby determining *n*, while the geometry determines the contact and interface morphology, thereby affecting the and *S*. Since the determined structure of OSM semiconductors can be selectively adjusted, these OSMs hold great promise as adhesives to achieve high performance. Among the four OSMSs, the 1,3,6,8-tetrakis(3,6-di-*tert*-butyl-9*H*-carbazol-9-yl)pyrene (TCzPy)-based composite films show the highest performance.

As good n-type thermoelectric materials, amino-substituted perylene diimides (PDINE) and naphthalene diimides (NDINE) have been reported quite recently. Gao *et al.* synthesized a variety of acridones with various terminal tertiary amine groups (ADTA) based on the molecular structures of PDINE and NDINE[53]. The number of side chains and the terminal tertiary amine had a significant impact on the thermoelectric performance of composites. The composite containing two terminal diethyl amine groups and an acridone had the highest PF of 289.4 ± 2.8 $\mu W \cdot m^{-1} \cdot K^{-2}$ at 430 K. It was shown that the π-π and cationic-π connections between OSMs and SWCNTs significantly improved the thermoelectric properties. Nevertheless, as thermoelectric materials, only a small number of OSMs with π and cationic structures have been composited with SWCNTs thus far. Li *et al.*, for the first time, used the OSMs with a cation group (benzotriazol-1-yloxy)tripyrrolidinophosphonium hexafluorophosphate (PyBOP) to compound with SWCNTs, and the interaction between SWCNTs and OSMs could significantly improve the thermoelectric performance of composites[54]. The findings indicate that modifying the OSM structure can greatly increase the σ of SWCNT composites, indicating a potential avenue for the quick creation of high-performance thermoelectric composite materials.

Twisted molecular structure

Twisted OSMs improve the thermoelectric performance of OSM/SWCNT composite films by significantly boosting the *S* and minimizing the inevitable decrease in σ. This is because the SWCNTs and OSMs have a little charge transfer interaction that encourages charge carrier transit between them. According to the research by Jeon *et al.*, the hybridization of SWCNTs with a twisted OSM N,N-diphenyl-4'-(1,2,2-triphenylvinyl)-[1,1'-biphenyl]-4-amine (TPETPA) greatly enhanced the thermoelectric performance of hybrid films[55]. The SWCNT/TPETPA film's *S* is increased and its decrease in σ is minimized because of the mild charge transfer contact between SWCNT bundles and TPETPA, which facilitate charge carrier transit between them, leading to high PF for the SWCNT/TPETPA@13.8 wt% film. Wei *et al.* present a range of innovative butterfly-like OSMs in which butterfly-shaped OSMs with deformed molecular structures and precisely adjusted frontier molecule orbitals are the key to this design[56]. When dense thiophenyl and carbonyl groups are added to the skeleton, the molecular structure is often distorted. This raises the activation energy *E*a and results in a high *S* for the butterfly-shaped molecule. Additionally, the twisting shape improved molecular contact with the SWCNT surface, raising the doping levels. At 350 K, the OSM/SWCNT composite films exhibit a maximum PF of 312 $\mu W \cdot m^{-1} \cdot K^{-2}$. According to these results, twisted OSMs show promise as a substitute for planar OSMs in the creation of high-performance OSMs/SWCNT thermoelectric materials.

Spiro molecular structure

Zhu *et al.* suggested a strategy to significantly improve the thermoelectric performance of SWCNTs by p-type doping of three spiro-OSMs[39]. The energy levels of OSMs were influenced by the addition of oxygen and sulfur heteroatoms, which led to an appropriate HOMO level that matched the E_F of SWCNTs. Doping and improving thermoelectric performance are thought to be accomplished through strong interfacial contact and evident electron transport. At ambient temperature, the composite film exhibits the greatest PF, about twice as high as that of pristine SWCNTs. Zhang *et al.* created a number of novel Spiro molecules that could be combined with SWCNTs as p-type thermoelectric materials[57]. They have an extended conjugated system that makes interaction with SWCNTs easier, in addition to a spiro carbon that contributes to the 3D structure and high solubility. The authors demonstrated that the interactions between OSMs and SWCNTs increase with the conjugation system. These interactions facilitate the transfer of electrons from the HOMO of OSMs to the E_F of SWCNTs. Consequently, the PF value of the OSM/SWCNT composites is almost twice that of the pristine SWCNTs. These works suggest that molecules with spiro structures compounded with SWCNTs are a promising p-type OTE material.

Reducing molecules and solvents

The p-type or n-type performance of CNT-based thermoelectric materials can be easily adjusted by adding oxidation-reducing agents. Borane-nitrogen derivatives (BNs) are often used as reducing agents to prepare n-type thermoelectric materials. Mao *et al.* investigated three BNs with varying reduction abilities (the structure is illustrated in Figure 4) as n-type dopants of SWCNTs by mixing BNs with SWCNTs in different solvents[58]. The findings indicate that borane complex structures and their capacity to reduce have a significant impact on thermoelectric performance. In the temperature range examined, SWCNT/ pyridineborane (PYB) demonstrated the highest level of performance. Nie *et al.* have developed a series of organometallic complexes with reducing ability and studied the influence of solvents on n-type SWCNT matrix composites[59]. The results showed that ferrocene derivatives and N-methyl pyrrolidone (NMP) worked in concert to improve the n-type features. The best thermoelectric performance was achieved by SWCNT/ *N,N'*-dimethylferrocenemethylamine (FcMA) made by NMP out of the three complexes; the maximum PF at ambient temperature was 567.54 ± 27.18 $\mu W \cdot m^{-1} \cdot K^{-2}$.

The solvent has a great influence on the electrical properties of n-type SWCNT-based composites[60]. According to Wang *et al.*, using an appropriate solvent can significantly improve the n-type electrical characteristics of SWCNT-based composites by promoting the conversion of their p-type to n-type[61]. At ambient temperature, the n-type σ of SWCNTs prepared in dimethyl sulfoxide (DMSO) (SWCNT/DMSO) was much higher than that of SWCNTs prepared in water (SWCNT/H_2O). Morphological characterization indicates that SWCNT/DMSO films contained porous structures for easy n-type doping. Theoretical calculation revealed that varying solvent polarity significantly impacted the surfactant wrapping morphology on SWCNTs, leading to diverse coating densities of SWCNT films. These variations, in turn, influenced n-type doping efficiency and n-type σ.

Preparation of air-stable n-type OSM/SWCNT materials

Encapsulation

In the study of n-type OSM/SWCNT materials, obtaining good stability is also an important goal researchers pursue. At present, some studies use polyethyleneimine (PEI) to dope CNTs, which can not only convert conventional p-type CNTs into n-type materials, but also construct an anoxic environment, hence maintaining the n-type stability of the material[62,63]. For n-type OSM/SWCNT thermoelectric materials, a similar encapsulation method can also be used to achieve the stability. Fukumaru *et al.* successfully achieved stable n-type doping by encapsulating $CoCp_2$ into SWCNTs[64]. For SWCNT films without $CoCp_2$ doping, oxygen doping in the air naturally exhibited p-type thermoelectric performance. However, when $CoCp_2$ was inserted inside SWCNTs, the doping of $CoCp_2$ caused the SWCNT film to exhibit n-type thermoelectric performance. In addition to the change of *S* symbol, the σ of $CoCp_2$@SWCNT films also increases significantly by nearly ten times, resulting in a significantly higher PF of n-type film than that of p-type film. Due to insertion (encapsulation) of $CoCp_2$ into the interior of SWCNTs, the SWCNTs themselves acted as an encapsulation material, blocking $CoCp_2$ and oxygen in the air, thereby resulting in stable n-type thermoelectric performance. Nonoguchi *et al.* successfully achieved stable n-type doping by encapsulating dppf into SWCNTs, and the PF exceeds approximately 240 $\mu W \cdot m^{-1} \cdot K^{-2}$[65]. By doping cationic surfactants, Hata *et al.* obtained high-efficient water-resistant n-type CNT composite thermoelectric materials[66,67].

Molecular structure regulation

Nonoguchi *et al.* impregnated SWCNT film in a mixture of salt (such as NaOH, KOH, KCl, etc.) and crown ether[21]. The cationic coordination of crown ether with alkali metal ($[M\text{-crown}]^+$, M = Li, Na, K) enabled n-type doping of SWCNTs. Experimental results show that SWCNT films doped with KOH and benz-18-crown-6-ether can maintain n-type properties at 100 °C for at least one month, as shown in Figure 5.

Figure 4. Structure of the three BNs. The figure is quoted with permission from Mao *et al.*[58]. PYB: Pyridineborane; DEANB: *N,N*-diethylanilineborane; MPB: morpholineborane.

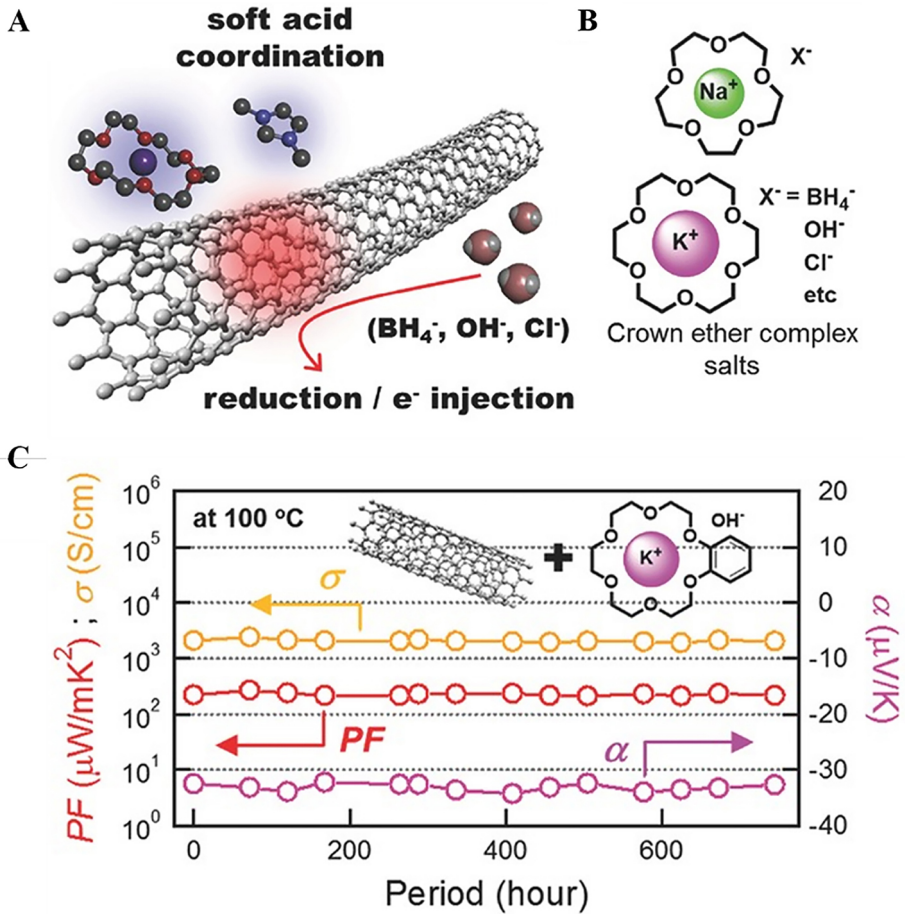

Figure 5. A: Schematic conceptualization of salt-induced n-type doping; B: the typical n-type dopants in this work; C: thermoelectric stability of KOH/benzo-18-crown ether at 100 °C. This figure is quoted with permission from Nonoguchi *et al.*[21].

Nonoguchi suggested that metal cations form [M-crown]$^+$ in the center of the crown ether, and OH^- reacts with SWCNTs to form hydrogen peroxide by electron transfer, thereby reducing SWCNTs and making it negatively charged. Halide anion Cl^- will form halogen molecules and provide electrons to SWCNTs, and halogen molecules can be removed by post-processing. While the anions achieve n-type doping, electron-rich SWCNTs attract cations [M-crown]$^+$ for charge compensation through electrostatic action, thus

achieving the role of stabilizing negative charge. Furthermore, the crown ether complex may prevent SWCNTs from directly adsorbing oxygen in air through crown ether, so as to improve the n-type stability of SWCNTs.

Nakashima *et al.* successfully developed an air-stable n-type SWCNT film by doping with 2-(2-methoxyphenyl)-1,3-dimethyl-2,3-dihydro-1H-benzo[d]imidazole (*o*-MeO-DMBI), showing exceptional air stability in an atmospheric environment[68]. X-ray photoelectron spectroscopy (XPS) and matrix-assisted laser desorption ionization-time of flight mass spectrometry (MALDI-TOF-MS) spectra reveal the formation of cations on the surface of SWCNTs, and the stable complex formed between cation dopants and anionic SWCNTs is considered a key factor in preventing air oxidation. He *et al.* fabricated a series of SWCNT/FcMA/polyethylene glycol (PEG) composite[69]. A synergistic effect might occur due to strong SWCNT-binding PEG and the high electron-donating FcMA. With long-term air stability, SWCNT/FcMA/PEG composites had the highest PF, reaching 600.6 ± 22.9 $\mu W \cdot m^{-1} \cdot K^{-2}$. The results of optical and morphological characterization show that PEG not only helps SWCNTs achieve outstanding air stability, but also inhibits SWCNTs from oxidizing. This work offers a workable and straightforward method for enhancing the air stability and thermoelectric performance of n-type OTE composite materials at the same time.

PREPARATION METHOD OF OSM/SWCNT COMPOSITES

There are many methods for the preparation of composites of OSMs and SWCNTs, including drop coating, vacuum filtration, micronizing mill process, and aerosol doping method, among which drop coating and vacuum filtration are commonly used.

Drop coating method

The most common method for compositing OSMs with SWCNTs is drop coating. The usual procedure is to disperse the OSMs and SWCNTs in a solvent under ultrasonication, ensuring the formation of a uniform mixture. The OSM/SWCNT composite films were produced by drop-casting the suspensions onto the glass surfaces under ambient circumstances after the glass substrates had been sonicated with solvent several times[47,70,71]. For example, the specific steps taken by Yin *et al.* in the preparation of 4,9-dihydro-sindaceno[1,2-b:5,6-b']dithiophene/SWCNT composite films using the drop coating method are as follows[40]. First, use a probe sonicator to disperse 30 mg of SWCNTs in 30 mL of chlorobenzene. Next, add various amounts of IDT to the dispersion to achieve different IDT/SWCNT ratios, and continuously stir the mixture. Proceed to ultrasonicate glass substrates separately in deionized water, acetone, and isopropanol, then drop-cast the suspension onto the glass substrates at room temperature to obtain a composite film.

Vacuum filtration method

The usual procedure is to disperse the OSMs and SWCNTs in a solvent and under ultrasonication to form an evenly dispersed mixture, and then use a qualitative filter paper for vacuum filtration to obtain an OSM/SWCNT composite film[72,73]. However, because OSMs are easily soluble in the solvent used, some OSMs will be lost during the filtration process. For example, the specific steps taken by Gao *et al.* in the preparation of SWCNT/ADTA thermoelectric materials using the vacuum filtration method are as follows. Adding SWCNTs to DMSO solution containing desired amount of ADTA. Sonicating the mixture until it is evenly dispersed. Subsequently, vacuum filter the mixture on a nylon membrane to obtain a composite film. Finally, vacuum drying the resulting film at 60 °C for 4 h[53].

Micronizing mill process method

Kang *et al.* utilized the micronizing mill process to easily produce a nanocomposite film made of various OSMs-supported small-bundle SWCNTs (SSWCNTs)[74]. The in-plane κ produced by π-π interactions in the

nanocomposite material can be efficiently decreased by the OSMs scattered throughout the SSWCNT film. Furthermore, without destroying or altering the SSWCNT structure, the micro powder grinding procedure guarantees uniform dispersion of small molecules and SSWCNTs. In order to uniformly disperse the organic materials in the SSWCNT matrix by exerting shear force on a plane, the precise stage was mixing OSMs and SSWCNTs in a homogeneous manner using a micronizing mill for 2 h. An OSM/SSWCNT slurry was prepared by dispersing OSMs and SSWCNTs in 1, 2-dichlorobenzene (ODCB) before the micronizing mill operation. The uniformly ground OSM/SSWCNT composite material was deposited on a 4 cm × 4 cm silicon mold polyimide substrate, evaporating the solvent, and removing the polyimide substrate to obtain an independent nanocomposite film with a thickness of approximately 30 μm.

Aerosol doping method

Recently, Khongthong *et al.* reported an aerosol technique to combine SWCNT film doping with real-time thermoelectric measurements[75]. Measuring as-generated thermoelectric voltage and resistivity by depositing aerosolized dopant solution onto preheated film. This technique ensures uniform doping and good scalability by combining superior control over doping parameters with thermoelectric performance tuning. The specific procedure involves atomizing the p-type doped solution of $HAuCl_4$ in isopropanol and the n-type doped solution of PEI in ethanol using an OMRON nebulizer separately, then directing the airflow onto the SWCNT film, as illustrated in Figure 6. After solvent evaporation, aerosol particles deposit on the nanotube film surface; concurrently, variations in the resistivity of the film and the produced thermoelectric voltage can be observed.

APPLICATIONS OF OSM/SWCNT COMPOSITES

A typical application for thermoelectric materials is in the fabrication of thermoelectric devices. TEGs are special power generation systems. A thermoelectric module with legs made of p-type and n-type materials that alternate and are coupled thermally in parallel and electrically in series. This leg-type arrangement is common in thermoelectric power generation because it facilitates heat movement inside the system and reduces parasitic losses from resistance[35]. SWCNT-based thermoelectric devices have great advantages in applications that collect low-grade heat. In particular, with the latest advancements in flexible and stretchable electronic devices, there is a significant demand for utilizing flexible TEGs. At present, SWCNT and polymer composite thermoelectric materials are widely used, including TEGs, textile electronic thermoelectric materials[76], sensors[77-79], supercapacitors[80], and so on. However, the main application of OSM/SWCNT thermoelectric materials is the fabrication of TEGs. Table 2 summarizes the performance of thermoelectric devices fabricated by OSM/SWCNT composite materials.

Kim *et al.* prepared flexible and lightweight OSM/SWCNT TEGs based on folding devices, which utilize the in-plane transport of SWCNTs[83]. In their study, the p-type composite achieved S of up to 97 $\mu V \cdot K^{-1}$. They utilized PEI and diethylenetriamine to reduce air-exposed SWCNTs, followed by treatment with $NaBH_4$ to convert them to n-type. Polytetrafluoroethylene insulating films were sandwiched between thermoelectric modules, which were coupled in an alternate fashion based on the optimal p-type and n-type OSM/SWCNT films. This layered construction (referred to as a module) had copper foil connecting it in series. The thermoelectric module consists of 72 pairs of p-n CNT films that can generate an open circuit voltage of 465 mV at a temperature gradient of 49 K.

Wu *et al.* converted the pristine SWCNTs (p-type) into n-type conductive material by DETA doping and treating with CaH_2 subsequently[84]. A possible mechanism is put forth to explain the conversion from p-type to n-type conduction. Using a multilayered alternating stacking structure to achieve high-property thermoelectric modules, it is possible to achieve series electrical conduction and parallel thermal

Table 2. The performance of TE devices based on OSM/SWCNT composites

Sample	n^a	*mb*	Voltage (mV)	Power (μW)	T^c (K)	Ref.
C8BTBT–F_4TCNQ/SWCNT	5	-	13.1	0.34[d]	38	[47]
SWCNT/FcMA	5	-	22.7	0.75[d]	54.1	[59]
SWCNT/PYB	5	-	28.8	1.15[d]	66	[58]
SWCNT/$NaBH_4$	5	-	23.7	0.79[d]	67	[58]
SWCNTs-8022-N-DMBI/DMSO	5	-	16	0.44[e]	60	[61]
NDI/SWCNT	5	-	30.4	2.81[d]	65	[70]
NDI-2T/SWCNT	5	-	30.3	0.94[d]	60	[71]
PDI-2T/SWCNT	5	-	38.2	0.92[d]	60	[71]
SWCNT/ADLA4	5	-	41.69	1.88[d]	74.8	[81]
SWCNT/Lys and SWCNT/Asp	5	-	42.3	4.3[d]	87	[82]
Spiro-MeOTAD/SWCNT	-	6	9.77	0.057[d]	30	[39]
2/SWCNT	-	10	16.6	2.08[d]	31	[56]
SFX/SWCNT	-	10	28.6	1.0[d]	60	[57]
pyrene/SSWCNT	-	20	20	1.5[d]	20	[74]
SWCNTs/dPhiz-6	-	5	16.5	3.2[d]	30	[38]

[a]the number of p–n junctions; [b]the number of p-type legs; [c]the temperature difference; [d]output power as a function of current; [e]output power as a function of load resistance. BTBT: [1]benzothieno[3,2-*b*][1]benzothiophene; F_4TCNQ: tetrafluorotetracyanoquinodimethane; SWCNT: single-walled carbon nanotubes; PYB: pyridineborane; DMSO: dimethyl sulfoxide; SSWCNT: small-bundle SWCNTs.

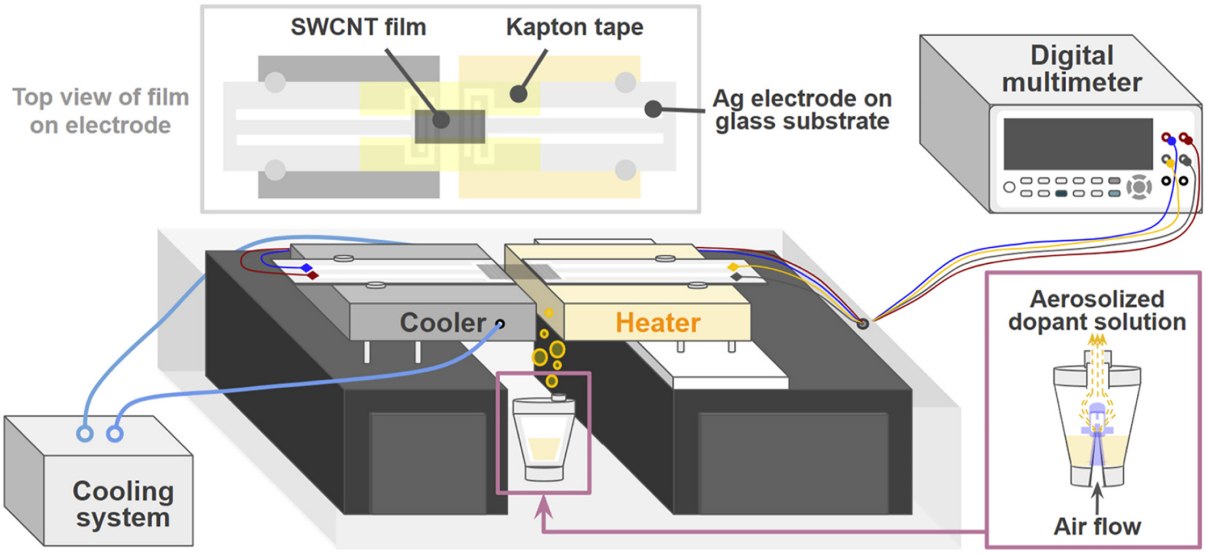

Figure 6. The setup diagram for doping a SWCNT film with aerosol in a closed box using thermoelectric monitoring in real time. This figure is quoted with permission from Khongthong *et al.*[75]. SWCNT: Single-walled carbon nanotube.

conduction, as shown in Figure 7. Finally, a total of 14 couples of thermoelectric modules exhibit large open-circuit voltages at temperature gradients of 55 and 110 K, measuring 62 and 125 mV, respectively. At these conditions, the maximum output power measured is 649 nW. The suggested approach creates a new avenue for the development of flexible devices with superior thermoelectric performance and organic n-type materials. Additionally, Wang *et al.* prepared highly ordered CNT films and achieved n-type doping through a vapor method, resulting in high-performance CNT composite films[85]. Based on this film, a

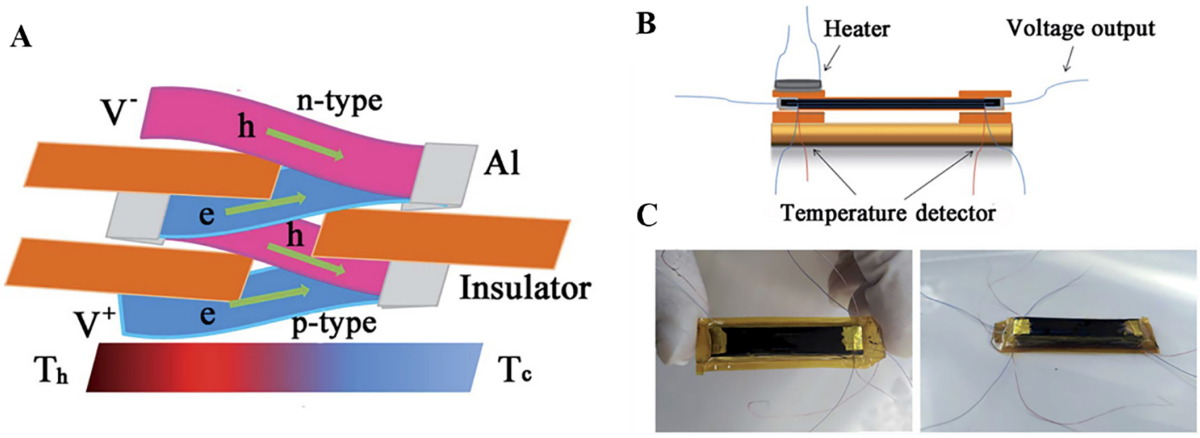

Figure 7. A: Diagram representing the multilayered, alternating, stacked structure of a module fitted. The heating and cooling ends are denoted by T_h and T_c, respectively, while the electrical connectors are Al foils; B: principle illustration of a working thermoelectric module; C: photo of thermoelectric module laminated with polyimide film. This figure is quoted with permission from Wu *et al.*[84].

curled TEG was developed, and the TEG was assembled to create an intelligent temperature controller, demonstrating the potential of organic CNT composite films in electronic temperature management applications[85].

CONCLUSIONS

This review summarizes the latest progress of OSM/SWCNT composite thermoelectric materials, including the optimization strategy of OSMs, preparation methods, and applications of OSM/SWCNT composites. In recent years, thanks to the development of new methods and technologies, OSM/SWCNT thermoelectric composite materials have made great progress in structural design and preparation methods. Some thermoelectric OSM/SWCNT composite materials have afforded high PFs comparable to the best semiconductor polymers, including both p-type and n-type materials. The n-type materials are still lagging behind compared to the p-type OSM/SWCNT materials, with probably the major cause of poor air stability. In-depth exploration of the relationship between OSMs and their performance is of great significance for enhancing thermoelectric performance of OSM/SWCNT composites. The theoretical construction of the relationship between structural changes and thermoelectric properties, such as energy level selection, conjugated skeleton modification, and customized side chain engineering, can provide guiding insights into further development. In the future, more OSMs need to be designed to explore the relationship between structure and thermoelectric performance. Further exploring and improving the preparation method of compositing OSMs and SWCNTs is also an effective way to improve the thermoelectric properties of OSM/SWCNT composites. Different preparation methods also have a great impact on the properties of thermoelectric composite materials. Along with the generation of interface, the composite system often affects the aggregation state of the material, carrier transport mechanism, etc., the potential phonon scattering at the interface, and the equivalent response of energy filtration also have a great impact on the thermoelectric parameters. Currently, applications of OSM/SWCNT composites mainly lie in the fabrication of TEGs, and the thermal management of electronic devices can be realized through TEG assembly in the future, which is beneficial for developing widely applied flexible thermoelectric devices. However, the practical application and commercial potential of OSM/SWCNT composites are far less than that of SWCNT/polymer composite thermoelectric materials, which still need to be further explored. From theoretical research to experimental studies, more efforts are still needed from researchers to accelerate the development of OSM/SWCNT composite materials, understanding their underlying mechanisms, and exploring the relationship between their structure and performance (molecular structure, morphology, etc.).

The study of OSM/SWCNT thermoelectric materials is an emerging and promising field, and it is reasonable to expect significant advances in thermoelectric properties in the future.

DECLARATIONS

Authors' contributions

Made substantial contributions to the conception and design of the study: Liu P, Guo CY
Performed data analysis and interpretation: Li Y
Conducted data interpretation: Ni Z

Availability of data and materials

Not applicable.

Financial support and sponsorship

None.

Conflicts of interest

All authors declared that there are no conflicts of interest.

Ethical approval and consent to participate

Not applicable.

Consent for publication

Not applicable.

REFERENCES

1. Laboratory LLN. Americans used more clean energy in 2016. Available from: https://www.llnl.gov/article/43246/americans-used-more-clean-energy-2016. [Last accessed on 13 Sep 2017].
2. Saleemi M, Toprak MS, Li S, Johnsson M, Muhammed M. Synthesis, processing, and thermoelectric properties of bulk nanostructured bismuth telluride (Bi_2Te_3). *J Mater Chem* 2012;22:725-30. DOI
3. Li JQ, Lu ZW, Wang CY, Li Y, Liu FS, Ao WQ. Enhanced thermoelectric properties of $Sn_{0.8}Pb_{0.2}Te$ alloy by Mn substitution. *Journal of Elec Materi* 2016;45:2879-85. DOI
4. Dong G, Zhu Y, Chen L. Microwave-assisted rapid synthesis of Sb_2Te_3 nanosheets and thermoelectric properties of bulk samples prepared by spark plasma sintering. *J Mater Chem* 2010;20:1976. DOI
5. Goldsmid HJ. Bismuth telluride and its alloys as materials for thermoelectric generation. *Materials (Basel)* 2014;7:2577-92. DOI PubMed PMC
6. Brostow W, Datashvili T, Hagg Lobland HE, et al. Bismuth telluride-based thermoelectric materials: coatings as protection against thermal cycling effects. *J Mater Res* 2012;27:2930-6. DOI
7. Liu F, Gong Z, Huang M, Ao W, Li Y, Li J. Enhanced thermoelectric properties of β-Cu_2Se by incorporating $CuGaSe_2$. *J Alloys Compd* 2016;688:521-6. DOI
8. Li J, Tang X, Li H, Yan Y, Zhang Q. Synthesis and thermoelectric properties of hydrochloric acid-doped polyaniline. *Synthetic Metals* 2010;160:1153-8. DOI
9. Bubnova O, Khan ZU, Malti A, et al. Optimization of the thermoelectric figure of merit in the conducting polymer poly(3,4-ethylenedioxythiophene). *Nat Mater* 2011;10:429-33. DOI PubMed
10. Bounioux C, Díaz-chao P, Campoy-quiles M, et al. Thermoelectric composites of poly(3-hexylthiophene) and carbon nanotubes with a large power factor. *Energy Environ Sci* 2013;6:918. DOI
11. Zhang L, Lin S, Hua T, Huang B, Liu S, Tao X. Fiber-based thermoelectric generators: materials, device structures, fabrication, characterization, and applications. *Adv Energy Mater* 2018;8:1700524. DOI
12. Wu H, Huang Y, Xu F, Duan Y, Yin Z. Energy harvesters for wearable and stretchable electronics: from flexibility to stretchability. *Adv Mater* 2016;28:9881-919. DOI PubMed
13. Beretta D, Massetti M, Lanzani G, Caironi M. Thermoelectric characterization of flexible micro-thermoelectric generators. *Rev Sci*

Instrum 2017;88:015103. DOI PubMed
14. Bahk J, Fang H, Yazawa K, Shakouri A. Flexible thermoelectric materials and device optimization for wearable energy harvesting. *J Mater Chem C* 2015;3:10362-74. DOI
15. Yao CJ, Zhang HL, Zhang Q. Recent progress in thermoelectric materials based on conjugated polymers. *Polymers (Basel)* 2019;11:107. DOI PubMed PMC
16. Xia B, Shi X, Zhang L, et al. Vertically designed high-performance and flexible thermoelectric generator based on optimized PEDOT:PSS/SWCNTs composite films. *Chem Eng J* 2024;486:150305. DOI
17. Wang Y, Dai X, Pan J, et al. Solvent effect induced charge polarity switching from p- to n-type in polyaniline and carbon nanotube hybrid films with a high thermoelectric power factor. *J Mater Chem A* 2024;12:18948-57. DOI
18. Huang J, Liu X, Du Y. Highly efficient and wearable thermoelectric composites based on carbon nanotube film/polyaniline. *Journal of Materiomics* 2024;10:173-8. DOI
19. Pernstich KP, Rössner B, Batlogg B. Field-effect-modulated seebeck coefficient in organic semiconductors. *Nat Mater* 2008;7:321-5. DOI PubMed
20. Germs WC, Guo K, Janssen RA, Kemerink M. Unusual thermoelectric behavior indicating a hopping to bandlike transport transition in pentacene. *Phys Rev Lett* 2012;109:016601. DOI PubMed
21. Nonoguchi Y, Nakano M, Murayama T, et al. Simple salt-coordinated n-type nanocarbon materials stable in air. *Adv Funct Materials* 2016;26:3021-8. DOI
22. Mistry KS, Larsen BA, Bergeson JD, et al. n-Type transparent conducting films of small molecule and polymer amine doped single-walled carbon nanotubes. *ACS Nano* 2011;5:3714-23. DOI PubMed
23. Chandra B, Afzali A, Khare N, El-ashry MM, Tulevski GS. Stable charge-transfer doping of transparent single-walled carbon nanotube films. *Chem Mater* 2010;22:5179-83. DOI
24. Hamid Elsheikh M, Shnawah DA, Sabri MFM, et al. A review on thermoelectric renewable energy: principle parameters that affect their performance. *Renew Sustain Energy Rev* 2014;30:337-55. DOI
25. Zhou D, Zhang H, Zheng H, et al. Recent advances and prospects of small molecular organic thermoelectric materials. *Small* 2022;18:e2200679. DOI PubMed
26. Drebushchak VA. The peltier effect. *J Therm Anal Calorim* 2008;91:311-5. DOI
27. Thomson W. 4. On a mechanical theory of thermo-electric currents. *Proc R Soc Edinb* 1857;3:91-8. DOI
28. Tritt TM, Subramanian MA. Thermoelectric materials, phenomena, and applications: a bird's eye view. *MRS Bull* 2006;31:188-98. DOI
29. She X, Su X, Du H, et al. High thermoelectric performance of higher manganese silicides prepared by ultra-fast thermal explosion. *J Mater Chem C* 2015;3:12116-22. DOI
30. Snyder GJ, Toberer ES. Complex thermoelectric materials. *Nat Mater* 2008;7:105-14. DOI PubMed
31. Liu FS, Zheng JX, Huang MJ, et al. Enhanced thermoelectric performance of $Cu_2CdSnSe_4$ by Mn doping: experimental and first principles studies. *Sci Rep* 2014;4:5774. DOI PubMed PMC
32. Blackburn JL, Barnes TM, Beard MC, et al. Transparent conductive single-walled carbon nanotube networks with precisely tunable ratios of semiconducting and metallic nanotubes. *ACS Nano* 2008;2:1266-74. DOI PubMed
33. Barnes TM, Blackburn JL, van de Lagemaat J, Coutts TJ, Heben MJ. Reversibility, dopant desorption, and tunneling in the temperature-dependent conductivity of type-separated, conductive carbon nanotube networks. *ACS Nano* 2008;2:1968-76. DOI PubMed
34. Nonoguchi Y, Ohashi K, Kanazawa R, et al. Systematic conversion of single walled carbon nanotubes into n-type thermoelectric materials by molecular dopants. *Sci Rep* 2013;3:3344. DOI PubMed PMC
35. Blackburn JL, Ferguson AJ, Cho C, Grunlan JC. Carbon-nanotube-based thermoelectric materials and devices. *Adv Mater* 2018:30. DOI PubMed
36. Kim T, Jang JG, Hong J. Enhanced thermoelectric performance of SWNT/organic small molecule (OSM) hybrid materials by tuning of the energy level of OSMs. *J Mater Chem C* 2020;8:12795-9. DOI
37. Kim TH, Hong JI. Energy level modulation of small molecules enhances thermoelectric performances of carbon nanotube-based organic hybrid materials. *ACS Appl Mater Interfaces* 2022;14:55627-35. DOI PubMed
38. Kim TH, Jang JG, Kim SH, Hong JI. Molecular engineering for enhanced thermoelectric performance of single-walled carbon nanotubes/π-conjugated organic small molecule hybrids. *Adv Sci (Weinh)* 2023;10:e2302922. DOI PubMed PMC
39. Zhu K, Hu Z, Chen G. Enhancement of thermoelectric property of carbon nanotubes by p-type doping with judicious molecular design of spiro-bifluorene derivatives. *Compos Commun* 2022;32:101166. DOI
40. Yin X, Zhong F, Chen Z, et al. Manipulating the doping level via host-dopant synergism towards high performance n-type thermoelectric composites. *Chemical Chem Eng J* 2020;382:122817. DOI
41. Gaul C, Hutsch S, Schwarze M, et al. Insight into doping efficiency of organic semiconductors from the analysis of the density of states in n-doped C_{60} and ZnPc. *Nat Mater* 2018;17:439-44. DOI PubMed
42. Wei P, Menke T, Naab BD, Leo K, Riede M, Bao Z. 2-(2-Methoxyphenyl)-1,3-dimethyl-1H-benzoimidazol-3-ium iodide as a new air-stable n-type dopant for vacuum-processed organic semiconductor thin films. *J Am Chem Soc* 2012;134:3999-4002. DOI PubMed
43. Bin Z, Li J, Wang L, Duan L. Efficient n-type dopants with extremely low doping ratios for high performance inverted perovskite solar cells. *Energy Environ Sci* 2016;9:3424-8. DOI

44. Sugiura H, Kanazawa Y, Nomura K, Aoai T. Fine tuning of the fermi level of single-walled carbon nanotubes with onium salts and application for thermoelectric materials. *Synthetic Metals* 2020;259:116222. DOI
45. Kim TH, Jang JG, Kim SH, Hong JI. Ambient-stable n-type carbon nanotube/organic small-molecule thermoelectrics enabled by energy level control. *ACS Appl Mater Interfaces* 2023;15:46872-80. DOI PubMed
46. Wang Y, Nakano M, Michinobu T, Kiyota Y, Mori T, Takimiya K. Naphthodithiophenediimide-Benzobisthiadiazole-based polymers: versatile n-type materials for field-effect transistors and thermoelectric devices. *Macromolecules* 2017;50:857-64. DOI
47. Qin S, Tan J, Qin J, et al. Benzothienobenzothiophene-based organic charge transfer complex and carbon nanotube composites for p-type and n-type thermoelectric materials and generators. *Adv Elect Materials* 2021;7:2100557. DOI
48. Jang JG, Hong J. Alkyl chain engineering for enhancing the thermoelectric performance of single-walled carbon nanotubes - small organic molecule hybrid. *ACS Appl Energy Mater* 2022;5:13871-6. DOI
49. Li P, Guo H, Xu H. Environmentally friendly ionic side chain organic small molecule/single-walled carbon nanotube composites have high TE performance. *J Mater Sci* 2022;57:18524-34. DOI
50. Jang JG, Kim T, Kim SH, Hong J. Enhancement of thermoelectric performance of single-walled carbon nanotubes/small organic molecule hybrids by fine-tuning of the alkyl chain length. *ACS Appl Electron Mater* 2023;5:5573-9. DOI
51. Zhou Y, Yin X, Liu Y, et al. Significantly enhanced power factors of p-type carbon nanotube-based composite films by tailoring the peripheral substituents in porphyrin. *ACS Sustainable Chem Eng* 2019;7:11832-40. DOI
52. Yin X, Peng Y, Luo J, et al. Tailoring the framework of organic small molecule semiconductors towards high-performance thermoelectric composites *via* conglutinated carbon nanotube webs. *J Mater Chem A* 2018;6:8323-30. DOI
53. Gao C, Liu Y, Gao Y, et al. High-performance n-type thermoelectric composites of acridones with tethered tertiary amines and carbon nanotubes. *J Mater Chem A* 2018;41:20161-9. DOI
54. Li B, Mao Y, Mao X, et al. Enhancement of the electrical conductivity and thermoelectric performance of single-walled carbon nanotubes by the introduction of conjugated small molecules with cation groups. *ACS Appl Energy Mater* 2020;3:11947-55. DOI
55. Jeon Y, Jang JG, Kim SH, Hong J. Twisted small organic molecules for high thermoelectric performance of single-walled carbon nanotubes/small organic molecule hybrids through mild charge transfer interactions. *J Mater Chem C* 2021;9:8483-8. DOI
56. Wei L, Huang H, Gao C, Liu D, Wang L. Novel butterfly-shaped organic semiconductor and single-walled carbon nanotube composites for high performance thermoelectric generators. *Mater Horiz* 2021;8:1207-15. DOI PubMed
57. Zhang L, Jin J, Huang S, et al. Cross-conjugated spiro molecules and single-walled carbon nanotubes composite for high-performance organic thermoelectric materials and generators. *Chem Eng J* 2021;426:131859. DOI
58. Mao X, Li Z, Liu Y, et al. Tuning the structure of borane-nitrogen derivatives towards high-performance carbon nanotubes-based n-type thermoelectric materials. *Chem Eng J* 2021;405:126616. DOI
59. Nie X, Mao X, Li X, et al. Combined effect of n-methyl pyrrolidone and ferrocene derivatives on thermoelectric performance of n-type single-wall carbon nanotube-based composites. *Chem Eng J* 2021;421:129718. DOI
60. Suzuki H, Kametaka J, Nakahori S, et al. N-DMBI doping of carbon nanotube yarns for achieving high n-type thermoelectric power factor and figure of merit. *Small Methods* 2024;8:e2301387. DOI PubMed
61. Wang Y, Li Q, Wang J, et al. Understanding the solvent effects on polarity switching and thermoelectric properties changing of solution-processable n-type single-walled carbon nanotube films. *Nano Energy* 2022;93:106804. DOI
62. Yu C, Murali A, Choi K, Ryu Y. Air-stable fabric thermoelectric modules made of n- and p-type carbon nanotubes. *Energy Environ Sci* 2012;5:9481. DOI
63. Xiao J, Zhang Z, Wang S, Gao C, Wang L. High-performance thermoelectric generator based on n-type flexible composite and its application in self-powered temperature sensor. *Chem Eng J* 2024;479:147569. DOI
64. Fukumaru T, Fujigaya T, Nakashima N. Development of n-type cobaltocene-encapsulated carbon nanotubes with remarkable thermoelectric property. *Sci Rep* 2015;5:7951. DOI PubMed PMC
65. Nonoguchi Y, Iihara Y, Ohashi K, Murayama T, Kawai T. Air-tolerant fabrication and enhanced thermoelectric performance of n-type single-walled carbon nanotubes encapsulating 1,1'-bis(diphenylphosphino)ferrocene. *Chem Asian J* 2016;11:2423-7. DOI PubMed
66. Hata S, Shiraishi M, Yasuda S, et al. Green route for fabrication of water-treatable thermoelectric generators. *Energy Mater Adv* 2022;2022:2022/9854657. DOI
67. Hata S, Maeshiro K, Shiraishi M, et al. Water-resistant organic thermoelectric generator with > 10 μW output. *Carbon Energy* 2022;5:e285. DOI
68. Nakashima Y, Nakashima N, Fujigaya T. Development of air-stable n-type single-walled carbon nanotubes by doping with 2-(2-methoxyphenyl)-1,3-dimethyl-2,3-dihydro-1 H -benzo[d]imidazole and their thermoelectric properties. *Synth Met* 2017;225:76-80. DOI
69. He G, Nie X, Cao G, et al. Achieving air-stable n-type single-walled carbon nanotubes with high thermoelectric performance by doping with polyethylene glycol and N,N-dimethylferrocenemethylamine. *Compos Sci Technol* 2023;238:110043. DOI
70. Wang Y, Chen Z, Huang H, Wang D, Liu D, Wang L. Organic radical compound and carbon nanotube composites with enhanced electrical conductivity towards high-performance p-type and n-type thermoelectric materials. *J Mater Chem A* 2020;8:24675-84. DOI
71. Liang J, Sun S, Huang S, et al. Boosting thermoelectric performance of carbon nanotube-based materials and devices by radical-containing molecules. *Mater Today Commun* 2023;35:106317. DOI
72. Wu G, Zhang ZG, Li Y, Gao C, Wang X, Chen G. Exploring high-performance n-type thermoelectric composites using amino-substituted rylene dimides and carbon nanotubes. *ACS Nano* 2017;11:5746-52. DOI PubMed

73. Cheng X, Wang X, Chen G. A convenient and highly tunable way to n-type carbon nanotube thermoelectric composite film using common alkylammonium cationic surfactant. *J Mater Chem A* 2018;6:19030-7. DOI
74. Kang YH, Lee Y, Lee C, Cho SY. Influence of the incorporation of small conjugated molecules on the thermoelectric properties of carbon nanotubes. *Org Electron* 2018;57:165-70. DOI
75. Khongthong J, Raginov NI, Khabushev EM, et al. Aerosol doping of SWCNT films with p- and n-type dopants for optimizing thermoelectric performance. *Carbon* 2024;218:118670. DOI
76. Serrano-Claumarchirant JF, Brotons-Alcázar I, Culebras M, et al. Electrochemical synthesis of an organic thermoelectric power generator. *ACS Appl Mater Interfaces* 2020;12:46348-56. DOI PubMed
77. Khan AAP, Khan A, Asiri AM, Alam MM, Rahman MM, Shaban M. Surfactant-assisted graphene oxide/methylaniline nanocomposites for lead ionic sensor development for the environmental remediation in real sample matrices. *Int J Environ Sci Technol* 2019;16:8461-70. DOI
78. Feng X, Li R, Ma Y, et al. One-step electrochemical synthesis of graphene/polyaniline composite film and its applications. *Adv Funct Materials* 2011;21:2989-96. DOI
79. Culebras M, López AM, Gómez CM, Cantarero A. Thermal sensor based on a polymer nanofilm. *Sens Actuators A Phys* 2016;239:161-5. DOI
80. Tong L, Jiang C, Cai K, Wei P. High-performance and freestanding PPy/Ti_3C_2Tx composite film for flexible all-solid-state supercapacitors. *J Power Sources* 2020;465:228267. DOI
81. Liu Y, Dai Q, Zhou Y, et al. High-performance n-type carbon nanotube composites: improved power factor by optimizing the acridine scaffold and tailoring the side chains. *ACS Appl Mater Interfaces* 2019;11:29320-9. DOI PubMed
82. Cao G, Nie X, Ren Z, et al. Simultaneously achieving green p- and n-type single-walled carbon nanotube composites by natural amino acids with high performance for thermoelectrics. *ACS Sustainable Chem Eng* 2022;10:12009-15. DOI
83. Kim SL, Choi K, Tazebay A, Yu C. Flexible power fabrics made of carbon nanotubes for harvesting thermoelectricity. *ACS Nano* 2014;8:2377-86. DOI PubMed
84. Wu G, Gao C, Chen G, Wang X, Wang H. High-performance organic thermoelectric modules based on flexible films of a novel n-type single-walled carbon nanotube. *J Mater Chem A* 2016;4:14187-93. DOI
85. Wang H, Li K, Hao X, et al. Capillary compression induced outstanding n-type thermoelectric power factor in CNT films towards intelligent temperature controller. *Nat Commun* 2024;15:5617. DOI PubMed PMC